Anti-plane shear waves in an elastic strip rigidly attached to an elastic half-space

Gennadi Mikhasev[a], Barış Erbaş[b], Victor A. Eremeyev[c,d,*]

[a] *Department of Bio- and Nanomechanics, Faculty of Mechanics and Mathematics, Belarusian State University, Nezavisimosty Ave., 4, 220030 Minsk, Belarus*
[b] *Department of Mathematics, Eskisehir Technical University Yunus Emre Campus, 26470, Eskisehir, Turkey*
[c] *Department of Civil and Environmental Engineering and Architecture (DICAAR), University of Cagliari, Via Marengo, 2, 09123 Cagliari, Italy*
[d] *Faculty of Civil and Environmental Engineering, Gdańsk University of Technology, ul. Gabriela Narutowicza 11/12 80-233 Gdańsk, Poland*

Abstract

We consider the anti-plane shear waves in a domain consisting of an infinite layer with thin coating lying on an elastic half-space. The elastic properties of the coating, layer, and half-space are assumed to be different. On the free upper surface we assume the compatibility condition within the Gurtin–Murdoch surface elasticity, whereas at the plane interface we consider perfect contact. For this problem there exist two possible regimes related to waves exponentially decaying in the half-space. The first one, called TE-TE regime, is related to waves described by exponential in transverse direction functions; the second, TH-TE regime, corresponds to waves in the upper layer which have the harmonic behaviour in the transverse direction. Detailed analysis of the derived dispersion equations for both regimes is provided. In particular, the effects of surface stresses, the layer thickness as well as of the ratio of shear moduli of the upper layer and half-space on the dispersion curves is analyzed.

Keywords: surface elasticity, anti-plane waves, dispersion relations, harmonic and exponentional regimes, elastic layer on a half-space

*Corresponding author.
Email addresses: mikhasev@bsu.by (Gennadi Mikhasev), berbas@eskisehir.edu.tr (Barış Erbaş), eremeyev.victor@gmail.com (Victor A. Eremeyev)

Introduction

Nowadays one can observe an essential extension of applications of continuum and structural mechanics towards description of material behaviour at small scales and towards more detailed analysis of new composite materials. Such an extension requires consistent modifications of classic mechanics. Among various enhancements of mechanics it is worth mentioning the surface elasticity approach. It is based on the introduction of additional constitutive relations defined at free surfaces or interfaces. The most popular models of surface elasticity relates to the seminal papers by Gurtin & Murdoch (1975, 1978) and by Steigmann & Ogden (1997, 1999). These models extend classic notion of surface tension by Laplace (1805, 1806); Young (1805); Longley & Van Name (1928) to finite deformations of elastic solids with material surfaces/interfaces. In particular, surface elasticity can describe so-called size-effects observed at the nanoscale, see *e.g.* Duan et al. (2008); Wang et al. (2011); Javili et al. (2013); Eremeyev (2016); Mogilevskaya et al. (2021a).

Let us note that the surface elasticity governing equations were introduced by direct approach, i.e. by postulation of existence of surface energy and surface stresses. But it could be also confirmed as a result of asymptotic analysis of so-called hard skins (Berdichevsky, 2010a,b) or stiff interfaces Benveniste & Miloh (2001, 2007), see extended discussions given by Gorbushin et al. (2020); Eremeyev et al. (2020). For example, within the linear Gurtin–Murdoch surface elasticity the boundary conditions on the interface coincide up to notations with the transmission condition on the stiff interface in the case of anti-plane deformations given by Mishuris et al. (2006b). So surface elasticity could be also useful for modelling of thin coatings or interface layers of finite thickness as discussed in Mishuris et al. (2006a, 2010); Sevostianov & Kachanov (2007).

After Korteweg (1901) and Mindlin (1965) it was also established that the surface elasticity is closely related to strain gradient elasticity, see *e.g.* Eremeyev et al. (2019), and to other nonlocal theories, see recent works by Chebakov et al. (2016); Ghayesh & Farajpour (2019); Li et al. (2020); Jiang et al. (2022b); Kaplunov et al. (2022); Yang et al. (2023). Similar surface-related phenomena could be results of deformations localization in the vicinity of a surface (Kaplunov & Prikazchikov, 2017; Kaplunov et al., 2019). More-

over, surface elasticity could be derived as a continuum limit of lattice dynamics if one assumes a certain scaling law as in (Eremeyev & Sharma, 2019). From the mathematical point of view, the surface elasticity approach has an advantage, since in this theory we have only modified boundary conditions whereas equation in the bulk remain in classic form.

Presence of surface stresses results in essential changes in effective properties of nanostructured materials, see Duan et al. (2008); Wang et al. (2011); Sevostianov et al. (2019); Nazarenko et al. (2019); Zheng et al. (2021); Kushch (2021); Mogilevskaya et al. (2021b); Jiang et al. (2022a); Kushch & Mogilevskaya (2022). Moreover, a surface bending resistance property of the Steigmann–Ogden model could also be essential (Han et al., 2018; Mogilevskaya et al., 2021a). For example, it was established that due to surface elasticity a nanoporous material could be even stiffer than its solid counterpart (Duan et al., 2008). Surface stresses affect a material response during nanoindetation that could be useful for determination of surface elastic moduli (Li & Mi, 2019; Argatov, 2022; Zemlyanova & White, 2022). Since surface energy results in non-classic boundary conditions often called the generalized Young–Laplace equation, they may essentially change stress singularity in the vicinity of defects such as crack tips (Kim et al., 2013; Gorbushin et al., 2020) or dislocations (Dai & Schiavone, 2019; Grekov & Sergeeva, 2020). In other words, surface elasticity may have essential influence on the strength and fracture of nanostructured materials Duan et al. (2008); Zemlyanova (2020); Piccolroaz et al. (2021); Zheng et al. (2021); Zheng & Mi (2021).

Finally, it is worth noting that surface energy and surface stresses affect significantly propagation of surface waves. In particular, it was discovered a new class of anti-plane surface waves which do not exist without surface effects (Xu & Fan, 2015; Eremeyev et al., 2016). They are similar to Love waves in classic elastodynamics (Achenbach, 1973). The provided analysis of these waves for a half-space and for a layer of finite thickness given by Zhu et al. (2019); Eremeyev (2020); Mikhasev et al. (2021, 2022) demonstrated an essential role of surface energy on the wave propagation. In particular new regimes of surface waves in an elastic layer were discussed by Mikhasev et al. (2022). Similar to the case of plane geometry, surface elasticity introduces new phenomena in waves in cylinders, see Chen et al. (2014); Xu & Fan (2016); Huang (2018); Eremeyev et al. (2020). These wave phenomena could be useful for nondestructive damage evaluation of thin coatings, for evaluation of surface properties including determination of surface elastic moduli, as well as for modelling of acoustic signal propagation in

nanowires and nanofilms.

Following Eremeyev et al. (2016); Mikhasev et al. (2022), in this paper we discuss anti-plane surface waves in a multilayered medium which consists of thin coating modelled within the Gurtin–Murdoch surface elasticity and an elastic layer of finite thickness perfectly attached to an elastic half-space (Fig. 1). From the physical point of view, this structure describes a three-layered medium with thickness of layers of different order of magnitude. For example, it may describe a thin film with modified surface properties attached to a substrate. The considered layered medium generalizes recent results by Mikhasev et al. (2022) towards more realistic behaviour of substrate, which is now deformable and can transmit waves.

The paper is organized as follows. In Section 1 we formulate the statement of the problem under consideration in the case of anti-plane motions. For the layer two types of solutions are possible that are expressed through exponential and harmonic (trigonometric) functions, respectively. We call these solutions transverse exponential (TE) and transverse harmonic (TH), respectively. As in (Eremeyev et al., 2016), for the half-space there is only exponentially decaying solutions. Detailed analysis of TE solutions is given in Section 2, whereas harmonic waves are analyzed in Section 3. Finally, in Section 4 we provide detailed analysis of dispersion curves.

1. Setting the problem within linear Gurtin-Murdoch surface elasticity

Let us consider a three-dimensional elastic isotropic plate-like body of thickness h rigidly attached to an elastic isotropic half-space. The origin of the used Cartesian coordinate system is chosen at the interface as shown in Fig. 1.

To study anti-plane waves we assume the vector of displacement $\mathbf{u}$ in the form, see, *e.g.*, Achenbach (1973),

$$\mathbf{u} = \mathbf{u}(x_1, x_2, x_3, t) = u(x_1, x_2, t)\mathbf{i}_3, \tag{1}$$

where t is time and $\mathbf{i}_i$ are the base vectors, $i = 1, 2, 3$, see Fig. 1. In what follows we restrict ourselves to isotropic homogeneous materials. So, using Hooke's law for the anti-plane shear in both the layer and half-space, we obtain

$$\begin{aligned} \boldsymbol{\sigma} =& 2\mu_j \mathbf{e} = \sigma_{13}(\mathbf{i}_1 \otimes \mathbf{i}_3 + \mathbf{i}_3 \otimes \mathbf{i}_1) + \sigma_{23}(\mathbf{i}_2 \otimes \mathbf{i}_3 + \mathbf{i}_3 \otimes \mathbf{i}_2), \\ \sigma_{13} =& 2\mu_j \varepsilon_{13}, \quad \sigma_{23} = 2\mu_j \varepsilon_{23}, \quad j = 1, 2, \end{aligned} \tag{2}$$

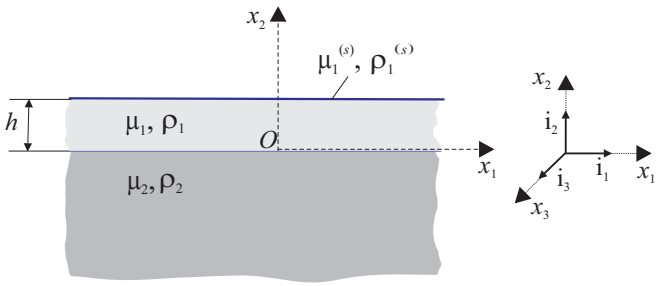

Figure 1: Infinite elastic plate-like domain lying on elastic half-space and used Cartesian coordinate system.

where $\boldsymbol{\sigma}$ and $\mathbf{e}$ are the stress and strain tensors, respectively, and μ_j is a shear modulus, which will be assumed to be different for the upper layer and half-space (μ_1 and μ_2, respectively). Hereinafter, the subscripts $j = 1$ and $j = 2$ correspond to the upper layer and half-space, respectively. Taking into account (1), the strain tensor reads

$$\begin{aligned} \mathbf{e} =& \varepsilon_{13}(\mathbf{i}_1 \otimes \mathbf{i}_3 + \mathbf{i}_3 \otimes \mathbf{i}_1) + \varepsilon_{23}(\mathbf{i}_2 \otimes \mathbf{i}_3 + \mathbf{i}_3 \otimes \mathbf{i}_2), \\ \varepsilon_{13} =& \frac{1}{2}\frac{\partial u}{\partial x_1}, \quad \varepsilon_{23} = \frac{1}{2}\frac{\partial u}{\partial x_2}. \end{aligned} \tag{3}$$

Here $\otimes$ stands for the dyadic product.

Taking into account the assumptions made, equations of motion for the two parts of the continuum take the form of wave equations Achenbach (1973)

$$\mu_j \left(\frac{\partial^2 u_j}{\partial x_1^2} + \frac{\partial^2 u_j}{\partial x_2^2} \right) = \rho_j \frac{\partial^2 u_j}{\partial t^2}, \quad j = 1, 2, \tag{4}$$

where ρ_j is the mass density in the bulk.

Below we consider the following boundary conditions. On the free surface $x_2 = h$, the compatibility condition within the Gurtin-Murdoch model of the surface elasticity is assumed as in Gurtin & Murdoch (1975, 1978):

$$\mu_1 \frac{\partial u_1}{\partial x_2} = \mu_1^{(s)} \frac{\partial^2 u_1}{\partial x_1^2} - \rho_1^{(s)} \frac{\partial^2 u_1}{\partial t^2} \quad \text{at } x_2 = h, \tag{5}$$

where $\mu_1^{(s)}$ and $\rho_1^{(s)}$ are surface shear modulus and density, respectively. At the interface $x_2 = 0$, we consider perfect contact which is expressed by two equations, namely,

$$u_1 = u_2 \qquad \text{at} \quad x_2 = 0, \tag{6}$$

$$\mu_1 \frac{\partial u_1}{\partial x_2} = \mu_2 \frac{\partial u_2}{\partial x_2} \qquad \text{at} \quad x_2 = 0. \tag{7}$$

Also, for the half-space, we set the wave attenuation condition at infinity,

$$u_2 \longrightarrow 0 \quad \text{as} \quad x_2 \longrightarrow -\infty. \tag{8}$$

In the recently published contribution by Mikhasev et al. (2022), an analysis of the wave equation for a thick plate with at least one free surface revealed the existence of two different regimes of anti-plane shear waves: (a) the TE regime for which waves decay exponentially from the upper and lower surfaces of the plate and (b) the TH regime with the harmonic behaviour of waves in the transverse direction. A similar analysis of Eqs. (4) for our problem shows that there exist both the TE and TH regimes in the plate and only the TE regime in the half-space. Here, we refer to these regimes as TE-TE and TH-TE, respectively.

2. TE-TE regime of anti-plane waves

Consider the TE-TE regime for which the amplitudes of anti-plane waves decay exponentially from the upper surface of the plate and from the interface in both directions. For this regime, a solution of Eqs. (4) can be sought in the form

$$u_1 = e^{i(kx_1-\omega t)}\left(a_1 e^{\alpha_1(x_2-h_1)} + a_2 e^{-\alpha_1 x_2}\right), \quad u_2 = b e^{i(kx_1-\omega t)} e^{\alpha_2 x_2}, \tag{9}$$

where $i = \sqrt{-1}$, k is a wave number, ω is the circular frequency, and a_1, a_2, b are constants that have to be determined from the boundary conditions.

Substituting (9) in Eqs. (4) for $j = 1, 2$, we find

$$\alpha_1 = |k|\sqrt{1 - c^2/c_{T1}^2}, \quad \alpha_2 = |k|\sqrt{1 - c^2/c_{T2}^2} \tag{10}$$

with

$$c = \frac{\omega}{k}, \quad c_{T1} = \sqrt{\frac{\mu_1}{\rho_1}} \quad \text{and} \quad c_{T2} = \sqrt{\frac{\mu_2}{\rho_2}}, \tag{11}$$

where c is the phase velocity, and c_{T1}, c_{T2} are the shear wave speeds in the upper layer and the half-space, respectively. Here, $c < c_{T1}$, $c < c_{T2}$.

Substituting (9) into the boundary conditions (5)–(7) and using (10), we arrive at the dispersion equation

$$\left(\frac{1}{|k|l_d}\sqrt{1-\frac{c^2}{c_{T1}^2}}+\frac{c_s}{c_{T1}^2}-\frac{c^2}{c_{T1}^2}\right)\left(\mu_2\sqrt{1-\frac{c^2}{c_{T2}^2}}+\mu_1\sqrt{1-\frac{c^2}{c_{T1}^2}}\right)$$
$$+\left(\frac{1}{|k|l_d}\sqrt{1-\frac{c^2}{c_{T1}^2}}-\frac{c_s}{c_{T1}^2}+\frac{c^2}{c_{T1}^2}\right)\left(\mu_2\sqrt{1-\frac{c^2}{c_{T2}^2}}\right. \tag{12}$$
$$\left.-\mu_1\sqrt{1-\frac{c^2}{c_{T1}^2}}\right)e^{-2|k|h_1\sqrt{1-c^2/c_{T1}^2}}=0$$

and the two relations for the required constants

$$a_1=\frac{\mu_1\alpha_1-\mu_1^{(s)}k^2+\rho_1^{(s)}\omega^2}{\mu_1\alpha_1+\mu_1^{(s)}k^2-\rho_1^{(s)}\omega^2}e^{-\alpha_1h_1}a_2,\quad b=\frac{\mu_1\alpha_1}{\mu_2\alpha_2}\left(a_1e^{-\alpha_1h_1}-a_2\right) \tag{13}$$

where

$$c_s=\sqrt{\frac{\mu_1^{(s)}}{\rho_1^{(s)}}},\quad l_d=\frac{\rho_1^{(s)}}{\rho_1}. \tag{14}$$

Here c_s is a shear wave speed in an elastic membrane associated to the Gurtin-Murdoch elasticity, and l_d is the so-called dynamic characteristic length.

Introducing the notations

$$m_{12}=\frac{\mu_1}{\mu_2},\quad k_d=|k|l_d,\quad h=nl_d, \tag{15}$$

and performing the scaling

$$v=\frac{c}{c_{T1}},\quad v_s=\frac{c_s}{c_{T1}},\quad v_r=\frac{c_{T2}}{c_{T1}}, \tag{16}$$

we get the dispersion equation written in the dimensionless form as follows

$$\left(\sqrt{1-\frac{v^2}{v_r^2}}+m_{12}\sqrt{1-v^2}\right)\left(\frac{1}{k_d}\sqrt{1-v^2}+v_s^2-v^2\right)$$
$$+\left(\sqrt{1-\frac{v^2}{v_r^2}}-m_{12}\sqrt{1-v^2}\right)\left(\frac{1}{k_d}\sqrt{1-v^2}-v_s^2+v^2\right)e^{-2nk_d\sqrt{1-v^2}}=0. \tag{17}$$

Let us consider some particular cases. If $m_{12} \to \infty$ (i.e., $\mu_2 \to 0$), then (17) degenerates into the equation (compare with Eq. (3.15) in Mikhasev et al. (2022))

$$\frac{1}{k_d}\sqrt{1-v^2} + v_s^2 - v^2 - \left(\frac{1}{k_d}\sqrt{1-v^2} - v_s^2 + v^2\right) e^{-2nk_d\sqrt{1-v^2}} = 0 \qquad (18)$$

for the layer with free bottom surface (see boundary condition (7)) without taking into account the surface effects.

On the other hand, when $m_{12} \to 0$, we arrive at the dispersion equation (see Eq. (3.7) in Mikhasev et al. (2022))

$$\frac{1}{k_d}\sqrt{1-v^2} + v_s^2 - v^2 + \left(\frac{1}{k_d}\sqrt{1-v^2} - v_s^2 + v^2\right) e^{-2nk_d\sqrt{1-v^2}} = 0 \qquad (19)$$

for the layer with the bottom layer clamped in the x_3-direction.

Passing to the limit as $n \to \infty$, we get the simple dispersion equation

$$\frac{1}{k_d}\sqrt{1-v^2} + v_s^2 - v^2 = 0 \qquad (20)$$

for the half-space with shear modulus μ_1 and density ρ_1.

Finally, if $n \to 0$, then we obtain the following simple equation

$$\frac{1}{k_d}\sqrt{1-\frac{v^2}{v_r^2}} + m_{12}(v_s^2 - v^2) = 0, \qquad (21)$$

which is similar to Eq. (20). Reverting to the initial dimensional variables, it is easy to show that the latter coincides with the same dispersion equation as in Eremeyev & Sharma (2019), see Eq. (5),

$$\frac{c^2}{c_{T2}^2} = \frac{c_s^2}{c_{T2}^2} + \frac{\rho_2}{|k|\rho_1^{(s)}}\sqrt{1-\frac{c^2}{c_{T2}^2}}, \qquad (22)$$

but for the half-space with shear modulus μ_2 and density ρ_2.

3. TH-TE regime of anti-plane waves

For the TH-TE regime, we seek solutions of Eqs. (4) in the form

$$u_1 = e^{i(kx_1-\omega t)}\left(a_1 \sin \lambda x_2 + a_2 \cos \lambda x_2\right), \quad u_2 = be^{i(kx_1-\omega t)}e^{\alpha x_2}, \qquad (23)$$

with a_1, a_2, b being constants.

Substituting (23) into Eqs. (4) gives

$$\lambda = |k|\sqrt{\frac{c^2}{c_{T1}^2} - 1}, \quad \alpha = |k|\sqrt{1 - \frac{c^2}{c_{T2}^2}}. \tag{24}$$

It can be seen that for the TH-TE regime $c_{T1} < c < c_{T2}$, i.e., the velocity of anti-plane shear wave is larger than the velocity of shear waves in the upper layer and less than the velocity of shear waves in the half-space.

Satisfying the boundary conditions (5)–(7) with (24) taken into account, we observe the following dispersion equation

$$\begin{aligned} &m_{12}\sqrt{\frac{c^2}{c_{T1}^2} - 1}\left(\sqrt{\frac{c^2}{c_{T1}^2} - 1}\tan\left(|k|h\sqrt{\frac{c^2}{c_{T1}^2} - 1}\right) - |k|l_d\left(\frac{c_s^2}{c_{T1}^2} - \frac{c^2}{c_{T1}^2}\right)\right) \\ &= \sqrt{1 - \frac{c^2}{c_{T2}^2}}\left(\sqrt{\frac{c^2}{c_{T1}^2} - 1} + |k|l_d\left(\frac{c_s^2}{c_{T1}^2} - \frac{c^2}{c_{T1}^2}\right)\tan\left(|k|h\sqrt{\frac{c^2}{c_{T1}^2} - 1}\right)\right) \end{aligned} \tag{25}$$

and the relations for the constants in (23) as

$$a_2 = b, \quad a_1 = \frac{\mu_2}{\mu_1}\frac{\alpha}{\lambda}b. \tag{26}$$

For the subsequent analysis, it is convenient to rewrite the dispersion Eq. (25) in the dimensionless form

$$\begin{aligned} &m_{12}\sqrt{v^2 - 1}\left(\sqrt{v^2 - 1}\tan\left(nk_d\sqrt{v^2 - 1}\right) - k_d\left(v_s^2 - v^2\right)\right) \\ &-\sqrt{1 - \frac{v^2}{v_r^2}}\left(\sqrt{v^2 - 1} + k_d\left(v_s^2 - v^2\right)\tan\left(nk_d\sqrt{v^2 - 1}\right)\right) = 0. \end{aligned} \tag{27}$$

We note that, in contrast to the TE-TE regime, Eq. (27) does not have any solution if the shear wave velocities of the upper layer and half-space coincide ($v_r = 1$). The limiting case when the upper layer degenerates into the half-space ($n \to \infty$) should also be excluded.

Let us consider again some particular cases. Let $m_{12} \to 0$. Then Eq. (27) admits a very simple form,

$$\tan\left(nk_d\sqrt{v^2 - 1}\right) = \frac{\sqrt{v^2 - 1}}{k_d\left(v^2 - v_s^2\right)}, \tag{28}$$

which coincides with equation (3.10) derived in Mikhasev et al. (2022) for the TH regime in the single layer with the bottom face clamped in the x_3-direction.

If $m_{12} \to \infty$, then we get the novel equation

$$\tan\left(nk_d\sqrt{v^2-1}\right) = -\frac{k_d\,(v^2-v_s^2)}{\sqrt{v^2-1}}, \tag{29}$$

which goes for TH regime in the single elastic layer with free bottom face without taking into account surface effects.

Finally, letting the upper layer vanish, i.e. $n \to 0$, we again arrive at Eq. (22), which is not valid for the TH regime, but can be used for the TE regime of the anti-plane waves in the half-space with the shear modulus μ_2 and the density ρ_2.

4. Dispersion curves analysis

4.1. TE-TE regime

Let us now consider the dispersion relation (17) corresponding to the TE-TE regime. First, we note that it has the root $v = 1$ (here $c = c_{T1}$) which should be excluded. Indeed, if $c = c_{T1}$, then $\alpha_1 = 0$ and, as follows from Eqs. (13), we get $u_1 = u_2 = 0$. Second, the numerical analysis of the dispersion Eq. (17) reveals that it does not have any positive roots if $v_r < 1$, i.e., for $c_{T1} > c_{T2}$. So, all subsequent calculations are performed for parameters satisfying the nonstrict inequality $c_{T1} \le c_{T2}$.

In Figure 2, the dimensionless velocity $v = c/c_{T1}$ versus the dimensionless wave parameter k_d is plotted at the fixed parameters $v_s = 0.25, m_{12} = 0.5, n = 20$ and for different values of the ratio $v_r = c_{T2}/c_{T1} = 1.005$, 1.01, 1.05, 1.1 (curves 1, 2, 3 and 4, respectively) of the shear waves velocities in the half-space and the upper layer. In Fig. 2 a), the dashed line corresponds to the case when the velocities of shear waves in the layer and half-space are the same, with mechanical properties being different. In the chosen scale, curve 4 merges with all dispersion curves for $v_r \ge 1.1$. Thus, the dashed line and the curve 4 can be considered as the lower and upper bounds, respectively, for the family of dispersion lines with different parameters v_r. Figure 2 b) shows that all dispersion curves asymptotically converge to the straight line $v = v_s$ (here, $v_s = 0.25$) as $k_d \to \infty$.

As expected, under fixed geometrical and physical parameters of the medium, the velocity c is a monotonically decreasing function of the wave

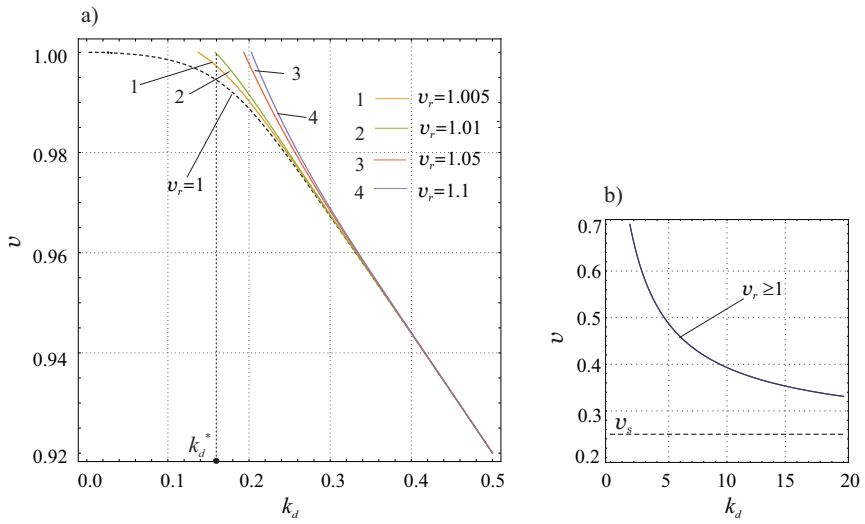

Figure 2: Dimensionless phase velocity $v = c/c_{T1}$ for TE-TE regime *vs.* wave number $k_d = |k|l_d$ for different ratios of the shear waves velocities in the half-space and the upper layer: a) Curves 1,2,3 and 4 correspond to ratios $v_r = 1.005$, 1.01, 1.05 and 1.1, respectively; the dashed curve marked by $v_r = 1$ corresponds to the case when the shear wave velocities in the upper layer and the half-space are the same; b) Dispersion curves for large values of k_d.

parameter k_d. It is also seen that increasing the shear wave velocity c_{T2} in the half-space results in increasing the velocity c of the anti-plane shear waves.

Another interesting observation coincides with similar results by Mikhasev et al. (2022): for any fixed speed ratio v_r, there exists such a wave parameter k_d^*, that Eq. (17) does not have solutions at the segment $k_d \in [0, k_d^*]$. The behaviour of the dispersion curve near the point $(k_d^*, 1)$ can be approximated by the linear function

$$v = 1 - A\xi + O(\xi^2) \quad \text{as} \quad \xi \to 0, \tag{30}$$

where $\xi = k_d - k_d^*$ with a parameter k_d^* to be determined and A is a constant.

Substituting (30) into Eq. (17) and equating coefficients in powers of $\xi^{1/2}$, we obtain the asymptotic relation for the point

$$k_d^* = \frac{\sqrt{m_{12}^2(1-v_s^2)^2 v_r^2 + 4n(1-v_s^2)(v_r^2-1)} - m_{12}v_r(1-v_s^2)}{2n(1-v_s^2)\sqrt{v_r^2-1}}. \tag{31}$$

The equation for the positive parameter A is not given here, since it is very cumbersome.

In Figure 3, the dispersion curves are drawn for $v_r = 2$, $v_s = 0.25, m_{12} = 0.5$ and different values of the parameter $n = h/l_d = h\rho_1/\rho_1^{(s)} = 0.025$, 0.25, 0.5, 1. The upper and lower dashed lines correspond to the cases when the elastic layer vanishes ($h \to 0$) or degenerates into a half-space ($h \to \infty$). These lines are plotted by solving Eqs. (21) and (20), respectively. It is seen

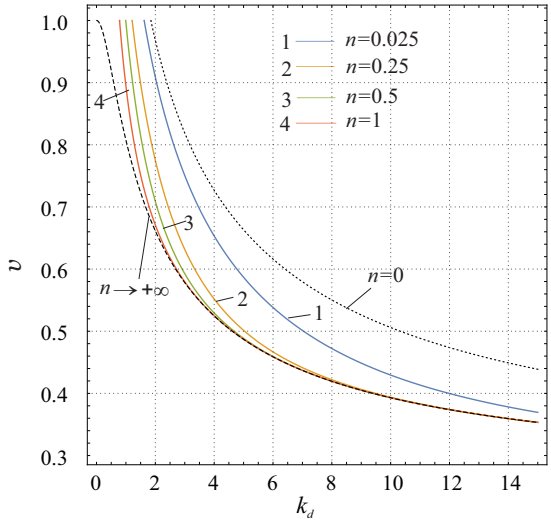

Figure 3: Dimensionless phase velocity $v = c/c_{T1}$ for TE-TE regime *vs.* wave number $k_d = |k|l_d$ for different values of the parameter $n = h/l_d = h\rho_1/\rho_1^{(s)} = 0.025,\ 0.25,\ 0.5,\ 1.1.$

that the velocity of anti-plane waves decreases when the thickness of the upper layer increases, and converges to the dashed line. Independent of the value of n, all curves converge to the straight line $v = v_s$.

Finally, Fig. 4 demonstrates the behaviour of the dispersion curves at different values of the ratio $m_{12} = \mu_1/\mu_2 = 0.5$, 1, 2, 5 and the fixed parameters $v_s = 0.25$, $n = 20$, $v_r = 2$. The upper and lower dashed lines plotted by solving Eqs. (19) and (18) are related to the limiting cases when $m_{12} \to 0$ and $m_{12} \to \infty$, respectively. It is of interest to note that the lower dashed line gives the phase velocities in the elastic layer with free surfaces, of which the upper one has the surface enhancement (within the Gurtin-Murdoch model), while the lower one does not.

4.2. TH-TE regime

Let us analyze the dispersion curves for the TH-TE regime. Figure 5 displays the solution of Eq. (27) with respect to v as a function of the

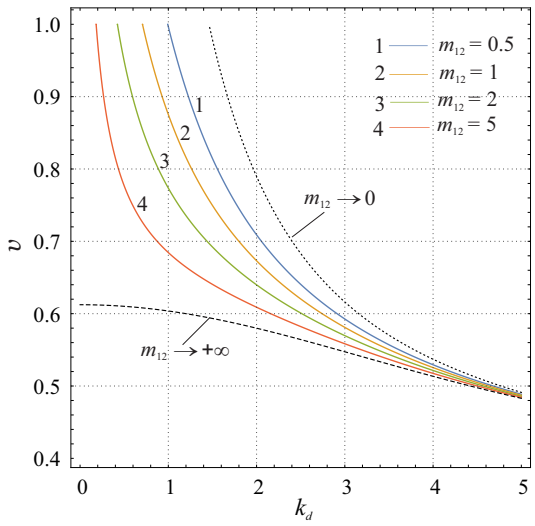

Figure 4: Dimensionless phase velocity $v = c/c_{T1}$ for TE-TE regime *vs.* wave number $k_d = |k|l_d$ for different values of the parameter $m_{12} = \mu_1/\mu_2 = 0.5,\ 1,\ 2,\ 5$.

wave parameter k_d for different values of the wave velocities ratio $v_r = 1.05, 1.1, 1.5, 1.5$. The calculations were performed at $v_s = 0.5$, $m_{12} = 0.5$, $n = 5$. The dashed curves correspond to the case when $v_r \to +\infty$. The curves lying above the straight line $v = 1$ are related to the TH-TE regime, while the curves below this line go for the TE-TE regime. It is of interest to note that the TE-TE curves plotted by solving Eq. (17) are continuations of the left family of the TH-TE curves.

In contrast to TE-TE regime, for each fixed value v_r there are the family (an infinite number) of the dispersion curves corresponding to TH-TE regime. Each dispersion line begins from some point (k_d^*, v_r) (which is removed). The point k_d^* is readily found by the asymptotic estimation of the dispersion curve behaviour in the neighbourhood of the point (k_d^*, v_r). Let

$$v = v_r - A\xi + O(\xi^2), \quad \xi = k - k_d^*. \tag{32}$$

We substitute (32) into Eq. (27) and expand all parameters depending on ξ into the series in powers of $\xi^{1/2}$. Considering only the leading approximation, we straightaway arrive at the equation with respect to the required k_d^*:

$$\tan\left(nk_d^*\sqrt{v_r^2 - 1}\right) = \frac{k_d^*(v_s^2 - v_r^2)}{\sqrt{v_r^2 - 1}}. \tag{33}$$

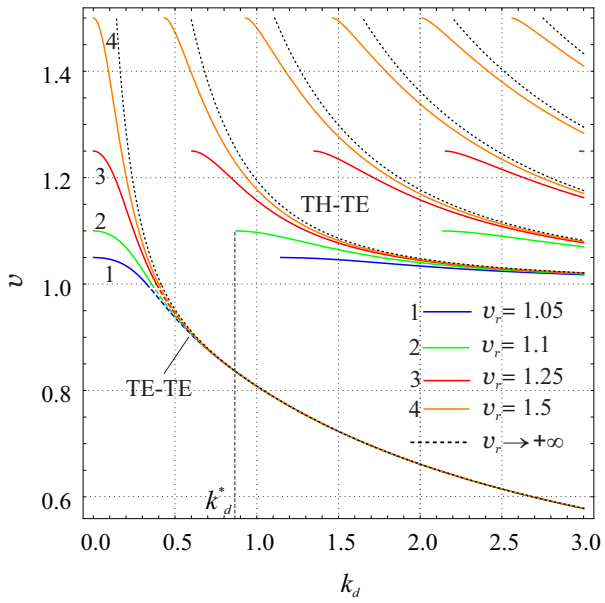

Figure 5: Dimensionless phase velocity $v = c/c_{T1}$ for TH-TE and TE-TE regimes *vs.* wave number $k_d = |k|l_d$ for different ratios of the shear waves velocities in the half-space and the upper layer. Curves 1,2,3, and 4 correspond to ratios $v_r = 1.005$, 1.1, 1.25 and 1.5, respectively. The dashed curves correspond to the limit case $v_r \to \infty$.

The constant A can be determined from the next two approximations, however because of cumbersome calculations we omit it here.

Figure 6 shows the behaviour of the dispersion curves, mainly for the TH-TE regimes, for different values of the parameter $n = 20, 10, 5$ (blue, green and red lines marked by 1, 2 and 3, respectively) specifying the thickness of the upper layer. Here the input parameters are the following: $v_s = 0.25, m_{12} = 0.5, v_r = 2$. The dashed black line, plotted by solving Eq. (22), is related to the case when the upper layer vanishes ($h \to 0$). We note that the left family of the TH-TE curves (which continuously transfer into the TE-TE lines below the straight line $v = 1$) starts from the point $(0, v_r)$ (here, $v_r = 2$) regardless of the thickness parameter n. The smaller the thickness h, the rarer the corresponding family of dispersion curves beginning from the point (k_d^*, v_r) with $k_d^* > 0$ becomes. In the limit, as $h \to 0$, all dispersion curves to the right of the dashed line and corresponding to only the TH-TE regime degenerate into this dashed line, which, however, is not a dispersion curve.

The effect of varying the elastic moduli ratio $m_{12} = \mu_1/\mu_2$ on the dimen-

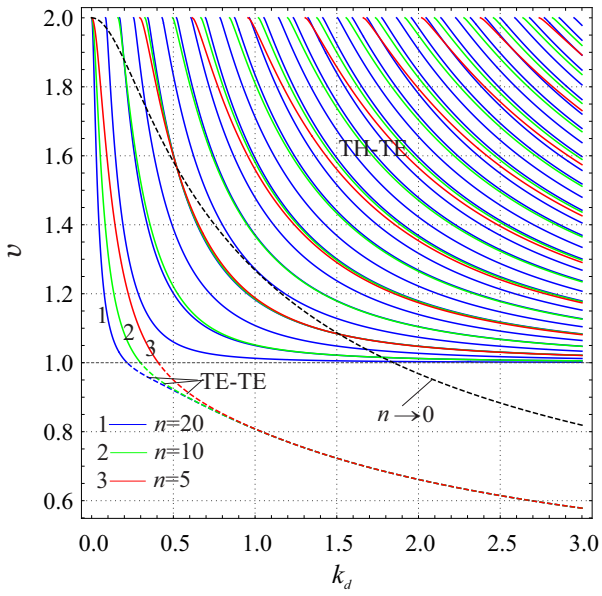

Figure 6: Dimensionless phase velocity $v = c/c_{T1}$ for TH-TE and TE-TE regimes *vs.* wave number $k_d = |k|l_d$ for different values of the parameter $n = 20, 10, 5$ (curves 1, 2, 3, respectively). The dashed black curve corresponds to the limit case $n \to 0$.

sionless phase velocity v is shown in Figure 7. The input parameters are $v_s = 0.25, n = 2$ and $v_r = 2$. The curves marked by 1, 2, 3 and 4 correspond to the ratios m_{12} equal to 0.03, 0.1, 1 and 2, respectively. The dashed black curves are related to the limit case as $m_{12} \to \infty$, and the black dash-dotted lines go for the case when $m_{12} \to 0$. The corresponding dispersion relations for these cases are Eqs. (29) and (28), respectively. The curves above and below the straight line $v = 1$ correspond to the TH-TE and TE-TE regimes, respectively. It may be seen that for the fixed values of the parameters v_s, n, v_r, the dispersion curves related to TH-TE regime for any ratio m_{12} get into one of the series of narrow domains which are bounded by the dashed and dash-dotted lines. The numerical experiments show that the thicker the elastic layer attached to the half-space (under other fixed input parameters), the more narrow each of these domains become. As $k_d \to \infty$, all curves related only to TH-TE regime together with the dashed and dash-dotted lines converge to the straight line $v = 1$, while the curves getting from the TH-TE regime into TE-TE one converge to the line v_s. Thus, with increasing wavenumber, the influence of the moduli ratio $m_{12} = \mu_1/\mu_2$ on the phase velocity c of the anti-plane waves weakens.

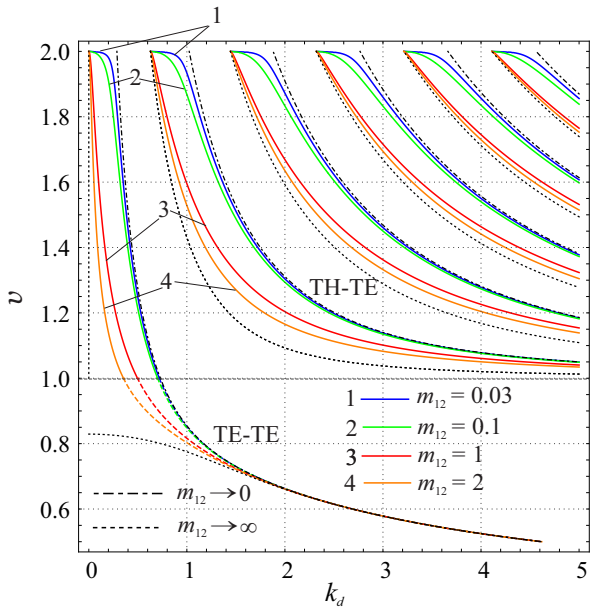

Figure 7: Dimensionless phase velocity $v = c/c_{T1}$ for TH-TE and TE-TE regimes *vs.* wave number $k_d = |k|l_d$ for different values of the parameter $m_{12} = 0.03, 0.1, 1, 2$ (blue, green, red and brown curves marked by 1, 2, 3, and 4, respectively). The dashed black curves correspond to the limit case when $m_{12} \to \infty$, and the black dash-dotted lines are related to the case $m_{12} \to 0$.

Conclusions

We discussed the propagation of anti-plane surface waves, i.e. waves localized in the vicinity of a free surface, in a layered elastic medium which consists of a layer of finite thickness perfectly attached to a half-space. In addition we also assume the action of surface stresses on the free surface of the layer. The Gurtin–Murdoch model is utilized here. The latter plays a crucial role here, since it corresponds to a new type of shear surface waves. We derived dispersion relations and presented the complete picture of dispersion curves. The presence of surface stresses brings additional characteristic length-scale parameters in the model. Accounting for the latter allowed detecting two novel regimes of anti-plane surface waves. The first one, called TE-TE regime corresponds to waves which exponentially decay in the transverse direction from both free and interface surfaces, while the second, TH-TE regime is related to waves which are specified by transversally harmonic (trigonometric) functions in the upper layer and by transversally exponential functions

in the half-space. It was observed that anti-plane waves in TE-TE regime propagate with lower speed than the ones in TH-TE regime. Since both regimes are determined by surface properties, these could be useful in the experimental determination of surface moduli as was proposed by Jia et al. (2018); Wu et al. (2020), and of surface material properties of multilayered coatings, in general.

Acknowledgments

G.M. acknowledges the support from the Scientific and Research Council of Turkey (TUBITAK) in the framework of Visiting Scientist Programme BIDEB 2221. V.A.E. acknowledges the support of the Royal Society Wolfson Visiting Fellowships program under the Project CR\212159 "Modelling of complex multiphysical phenomena on microstructured surfaces".

References

Achenbach, J. (1973). *Wave Propagation in Elastic Solids*. Amsterdam: North Holland.

Argatov, I. (2022). The surface tension effect revealed via the indentation scaling index. *International Journal of Engineering Science*, *170*, 103593.

Benveniste, Y., & Miloh, T. (2001). Imperfect soft and stiff interfaces in two-dimensional elasticity. *Mechanics of Materials*, *33*, 309–323.

Benveniste, Y., & Miloh, T. (2007). Soft neutral elastic inhomogeneities with membrane-type interface conditions. *Journal of Elasticity*, *88*, 87–111.

Berdichevsky, V. L. (2010a). An asymptotic theory of sandwich plates. *International Journal of Engineering Science*, *48*, 383–404.

Berdichevsky, V. L. (2010b). Nonlinear theory of hard-skin plates and shells. *International Journal of Engineering Science*, *48*, 357–369.

Chebakov, R., Kaplunov, J., & Rogerson, G. A. (2016). Refined boundary conditions on the free surface of an elastic half-space taking into account non-local effects. *Proceedings of the Royal Society A: Mathematical, Physical and Engineering Sciences*, *472*, 20150800.

Chen, W. Q., Wu, B., Zhang, C. L., & Zhang, C. (2014). On wave propagation in anisotropic elastic cylinders at nanoscale: surface elasticity and its effect. *Acta Mechanica*, *225*, 2743–2760.

Dai, M., & Schiavone, P. (2019). Edge dislocation interacting with a Steigmann–Ogden interface incorporating residual tension. *International Journal of Engineering Science*, *139*, 62–69.

Duan, H. L., Wang, J., & Karihaloo, B. L. (2008). Theory of elasticity at the nanoscale. In *Adv. Appl. Mech.* (pp. 1–68). Elsevier volume 42.

Eremeyev, V. A. (2016). On effective properties of materials at the nano- and microscales considering surface effects. *Acta Mechanica*, *227*, 29–42.

Eremeyev, V. A. (2020). Strongly anisotropic surface elasticity and antiplane surface waves. *Philosophical Transactions of the Royal Society A*, *378*, 20190100.

Eremeyev, V. A., Rosi, G., & Naili, S. (2016). Surface/interfacial anti-plane waves in solids with surface energy. *Mechanics Research Communications*, *74*, 8–13.

Eremeyev, V. A., Rosi, G., & Naili, S. (2019). Comparison of anti-plane surface waves in strain-gradient materials and materials with surface stresses. *Mathematics and Mechanics of Solids*, *24*, 2526–2535.

Eremeyev, V. A., Rosi, G., & Naili, S. (2020). Transverse surface waves on a cylindrical surface with coating. *International Journal of Engineering Science*, *147*, 103188.

Eremeyev, V. A., & Sharma, B. L. (2019). Anti-plane surface waves in media with surface structure: Discrete vs. continuum model. *International Journal of Engineering Science*, *143*, 33–38.

Ghayesh, M. H., & Farajpour, A. (2019). A review on the mechanics of functionally graded nanoscale and microscale structures. *International Journal of Engineering Science*, *137*, 8–36.

Gorbushin, N., Eremeyev, V. A., & Mishuris, G. (2020). On stress singularity near the tip of a crack with surface stresses. *International Journal of Engineering Science*, *146*, 103183.

Grekov, M. A., & Sergeeva, T. S. (2020). Interaction of edge dislocation array with bimaterial interface incorporating interface elasticity. *International Journal of Engineering Science*, *149*, 103233.

Gurtin, M. E., & Murdoch, A. I. (1975). A continuum theory of elastic material surfaces. *Arch. Ration. Mech. An.*, *57*, 291–323.

Gurtin, M. E., & Murdoch, A. I. (1978). Surface stress in solids. *Int. J. Solids Struct.*, *14*, 431–440.

Han, Z., Mogilevskaya, S. G., & Schillinger, D. (2018). Local fields and overall transverse properties of unidirectional composite materials with multiple nanofibers and Steigmann–Ogden interfaces. *International Journal of Solids and Structures*, *147*, 166–182.

Huang, Z. (2018). Torsional wave and vibration subjected to constraint of surface elasticity. *Acta Mechanica*, *229*, 1171–1182.

Javili, A., McBride, A., & Steinmann, P. (2013). Thermomechanics of solids with lower-dimensional energetics: on the importance of surface, interface, and curve structures at the nanoscale. A unifying review. *Applied Mechanics Reviews*, *65*, 010802.

Jia, F., Zhang, Z., Zhang, H., Feng, X.-Q., & Gu, B. (2018). Shear horizontal wave dispersion in nanolayers with surface effects and determination of surface elastic constants. *Thin Solid Films*, *645*, 134–138.

Jiang, Y., Li, L., & Hu, Y. (2022a). A compatible multiscale model for nanocomposites incorporating interface effect. *International Journal of Engineering Science*, *174*, 103657.

Jiang, Y., Li, L., & Hu, Y. (2022b). A nonlocal surface theory for surface–bulk interactions and its application to mechanics of nanobeams. *International Journal of Engineering Science*, *172*, 103624.

Kaplunov, J., Prikazchikov, D., & Sultanova, L. (2019). Rayleigh-type waves on a coated elastic half-space with a clamped surface. *Philosophical Transactions of the Royal Society A*, *377*, 20190111.

Kaplunov, J., & Prikazchikov, D. A. (2017). Asymptotic theory for Rayleigh and Rayleigh-type waves. *Advances in Applied Mechanics*, *50*, 1–106.

Kaplunov, J., Prikazchikov, D. A., & Prikazchikova, L. (2022). On non-locally elastic Rayleigh wave. *Philosophical Transactions of the Royal Society A*, *380*, 20210387.

Kim, C. I., Ru, C. Q., & Schiavone, P. (2013). A clarification of the role of crack-tip conditions in linear elasticity with surface effects. *Mathematics and Mechanics of Solids*, *18*, 59–66.

Korteweg, D. J. (1901). Sur la forme que prennent les équations des mouvements des fluides si l'on tient compte des forces capillaires par des variations de densité. *Archives Néerlandaises des sciences exactes et naturelles*, *Sér. II*, 1–24.

Kushch, V. I. (2021). Ellipsoidal inhomogeneity with anisotropic incoherent interface. multipole series solution and application to micromechanics. *International Journal of Engineering Science*, *168*, 103548.

Kushch, V. I., & Mogilevskaya, S. G. (2022). On modeling of elastic interface layers in particle composites. *International Journal of Engineering Science*, (p. 103697).

Laplace, P. S. (1805). Sur l'action capillaire. In *Supplément au livre X du Traité de mécanique céleste* (pp. 771–777). Paris: Gauthier–Villars et fils volume 4. Supplement 1, Livre X.

Laplace, P. S. (1806). Supplément à la théorie de l'action capillaire. In *Traité de mécanique céleste* (pp. 909–945). Paris: Gauthier–Villars et fils volume 4. Supplement 2, Livre X.

Li, L., Lin, R., & Ng, T. Y. (2020). Contribution of nonlocality to surface elasticity. *International Journal of Engineering Science*, *152*, 103311.

Li, X., & Mi, C. (2019). Effects of surface tension and Steigmann–Ogden surface elasticity on hertzian contact properties. *International Journal of Engineering Science*, *145*, 103165.

Longley, W. R., & Van Name, R. G. (Eds.) (1928). *The Collected Works of J. Willard Gibbs, PHD., LL.D.* volume I Thermodynamics. New York: Longmans.

Mikhasev, G. I., Botogova, M. G., & Eremeyev, V. A. (2021). On the influence of a surface roughness on propagation of anti-plane short-length localized waves in a medium with surface coating. *International Journal of Engineering Science*, *158*, 103428.

Mikhasev, G. I., Botogova, M. G., & Eremeyev, V. A. (2022). Anti-plane waves in an elastic thin strip with surface energy. *Phil. Trans. R. Soc. A*, *380*, 20210373–15.

Mindlin, R. D. (1965). Second gradient of strain and surface-tension in linear elasticity. *International Journal of Solids and Structures*, *1*, 417–438.

Mishuris, G., Öchsner, A., & Kuhn, G. (2006a). FEM-analysis of nonclassical transmission conditions between elastic structures. Part 2: Stiff imperfect interface. *CMC: Computers, Materials, & Continua,*, *4*, 137–152.

Mishuris, G. S., Movchan, N. V., & Movchan, A. B. (2006b). Steady-state motion of a Mode-III crack on imperfect interfaces. *The Quarterly Journal of Mechanics & Applied Mathematics*, *59*, 487–516.

Mishuris, G. S., Movchan, N. V., & Movchan, A. B. (2010). Dynamic Mode-III interface crack in a bi-material strip. *International Journal of Fracture*, *166*, 121–133.

Mogilevskaya, S. G., Zemlyanova, A. Y., & Kushch, V. I. (2021a). Fiber- and particle-reinforced composite materials with the Gurtin–Murdoch and Steigmann–Ogden surface energy endowed interfaces. *Applied Mechanics Reviews*, *73*, 1–18.

Mogilevskaya, S. G., Zemlyanova, A. Y., & Mantič, V. (2021b). The use of the Gurtin–Murdoch theory for modeling mechanical processes in composites with two–dimensional reinforcements. *Composites Science and Technology*, *210*, 108751.

Nazarenko, L., Chirkov, A. Y., Stolarski, H., & Altenbach, H. (2019). On modeling of carbon nanotubes reinforced materials and on influence of carbon nanotubes spatial distribution on mechanical behavior of structural elements. *International Journal of Engineering Science*, *143*, 1–13.

Piccolroaz, A., Peck, D., Wrobel, M., & Mishuris, G. (2021). Energy release rate, the crack closure integral and admissible singular fields in fracture mechanics. *International Journal of Engineering Science*, *164*, 103487.

Sevostianov, I., & Kachanov, M. (2007). Effect of interphase layers on the overall elastic and conductive properties of matrix composites. applications to nanosize inclusion. *International Journal of Solids and Structures*, *44*, 1304–1315.

Sevostianov, I., Mogilevskaya, S., & Kushch, V. (2019). Maxwell's methodology of estimating effective properties: Alive and well. *International Journal of Engineering Science*, *140*, 35–88.

Steigmann, D. J., & Ogden, R. W. (1997). Plane deformations of elastic solids with intrinsic boundary elasticity. *Proc. Roy. Soc. A: Mathematical, Physical and Engineering Sciences*, *453*, 853–877.

Steigmann, D. J., & Ogden, R. W. (1999). Elastic surface-substrate interactions. *Proc. Roy. Soc. A: Mathematical, Physical and Engineering Sciences*, *455*, 437–474.

Wang, J., Huang, Z., Duan, H., Yu, S., Feng, X., Wang, G., Zhang, W., & Wang, T. (2011). Surface stress effect in mechanics of nanostructured materials. *Acta Mech. Solida Sin.*, *24*, 52–82.

Wu, W., Zhang, H., Jia, F., Yang, X., Liu, H., Yuan, W., Feng, X.-Q., & Gu, B. (2020). Surface effects on frequency dispersion characteristics of Lamb waves in a nanoplate. *Thin Solid Films*, *697*, 137831.

Xu, L., & Fan, H. (2016). Torsional waves in nanowires with surface elasticity effect. *Acta Mechanica*, *227*, 1783–1790.

Xu, X., L. Wang, & Fan, H. (2015). Anti-plane waves near an interface between two piezoelectric half-spaces. *Mechanics Research Communications*, *67*, 8–12.

Yang, W., Wang, S., Kang, W., Yu, T., & Li, Y. (2023). A unified high-order model for size-dependent vibration of nanobeam based on nonlocal strain/stress gradient elasticity with surface effect. *International Journal of Engineering Science*, *182*, 103785.

Young, T. (1805). An essay on the cohesion of fluids. *Philosophical Transactions of the Royal Society of London*, *95*, 65–87.

Zemlyanova, A. Y. (2020). Interaction of multiple plane straight fractures in the presence of the Steigmann–Ogden surface energy. *SIAM Journal on Applied Mathematics*, *80*, 2098–2119.

Zemlyanova, A. Y., & White, L. M. (2022). Axisymmetric frictionless indentation of a rigid stamp into a semi-space with a surface energetic boundary. *Mathematics and Mechanics of Solids*, *27*, 334–347.

Zheng, C., & Mi, C. (2021). On the macroscopic strength criterion of ductile nanoporous materials. *International Journal of Engineering Science*, *162*, 103475.

Zheng, C., Zhang, G., & Mi, C. (2021). On the strength of nanoporous materials with the account of surface effects. *International Journal of Engineering Science*, *160*, 103451.

Zhu, F., Pan, E., Qian, Z., & Wang, Y. (2019). Dispersion curves, mode shapes, stresses and energies of SH and Lamb waves in layered elastic nanoplates with surface/interface effect. *International Journal of Engineering Science*, *142*, 170–184.